



The following Communications have been judged by at least two referees to be “very important papers” and will be published online at www.angewandte.org soon:

X. Lang, H. Ji, C. Chen, W. Ma,* J. Zhao*

Selective Formation of Imines by Aerobic Photocatalytic Oxidation of Amines on TiO₂

R. P. Sonawane, V. Jheengut, C. Rabalakos, R. Larouche-Gauthier, H. K. Scott, V. K. Aggarwal*

Enantioselective Construction of Quaternary Stereogenic Centers from Tertiary Boronic Esters: Methodology and Applications

K. Press, A. Cohen, I. Goldberg, V. Venditto, M. Mazzeo, M. Kol*

Salalen–Titanium Complexes for the Highly Isospecific Polymerization of 1-Hexene and Propylene

K. Nakano, S. Hashimoto, M. Nakamura, T. Kamada, K. Nozaki*
Synthesis of Stereogradient Poly(propylene carbonate) by Stereo- and Enantioselective Copolymerization of Propylene Oxide with Carbon Dioxide

D. Portehault,* S. Devi, P. Beaunier, C. Gervais, C. Giordano, C. Sanchez, M. Antonietti

A General Solution Route toward Metal Boride Nanocrystals

K. Ohmori, T. Shono, Y. Hatakoshi, T. Yano, K. Suzuki*

An Integrated Synthetic Strategy for Higher Catechin Oligomers



“My favorite subject at school was certainly not sports. The three qualities that make a good scientist are curiosity, creativity, and dedication ...”

This and more about Alois Fürstner can be found on page 2880.

Author Profile

Alois Fürstner _____ 2880–2882



H. B. Kagan



G. Bertrand



B. Chaudret



M. Antonietti



R. Poli

News

Blaise Pascal Medal: H. B. Kagan – 2883

Le Bel Prize: G. Bertrand _____ 2883

Süe Prize: B. Chaudret _____ 2883

Franco–German Prize:
M. Antonietti _____ 2883

Coordination Chemistry Prize:
R. Poli _____ 2884

William von Eggers Doering (1917–2011)

Obituaries

F.-G. Klärner _____ 2885–2886

Books

Enantioselective Chemical Synthesis

Elias J. Corey, László Kürti

reviewed by H.-G. Schmalz _____ 2887

4D Electron Microscopy

Ahmed H. Zewail, John M. Thomas

reviewed by G. Van Tendeloo _____ 2888

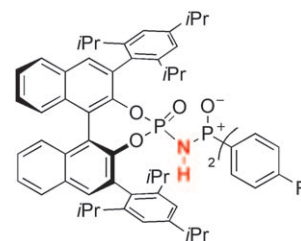
Highlights

Brønsted Acid Catalysis

J. N. Johnston* — 2890–2891

A Chiral *N*-Phosphinyl Phosphoramidate:
Another Offspring for the Sage
Phosphoric Acid Progenitor

Nitrogen enriched: The continuing quest for Brønsted acid catalysts that address unmet selectivity needs in organic synthesis has resulted in a new chiral phosphoric acid derivative. At the heart of this catalyst is a hydrogen-bond donor (N–H) that promotes an enantioselective intramolecular addition of oxygen (OH) to an azomethine (C=N). Diversity within a privileged chiral architecture invariably leads to new catalytic enantioselective chemical reactions.



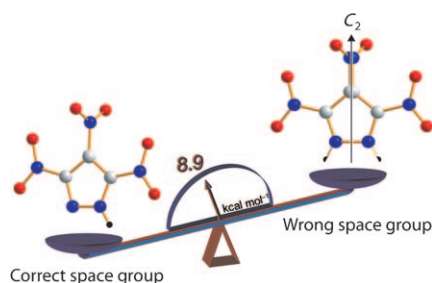
Correspondence

Structure Elucidation

Y. V. Nelyubina, I. L. Dalinger,
K. A. Lyssenko* — 2892–2894



Pseudosymmetry in Trinitropyrazole:
The Cost of Error in Space-Group
Determination



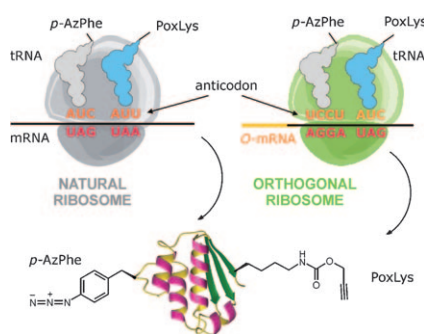
Trial and error: Topological analysis of the experimental electron density distribution of trinitropyrazole has allowed the energetic consequences of an overlooked pseudosymmetry to be quantified for the first time. This has allowed measurement of how much a small error in the assignment of a space group may cost a crystal structure; in the case of trinitropyrazole this was 8.9 kcal mol^{−1}.

Minireviews

Expansion of the Genetic Code

M. G. Hoesl, N. Budisa* — 2896–2902

In Vivo Incorporation of Multiple
Noncanonical Amino Acids into Proteins

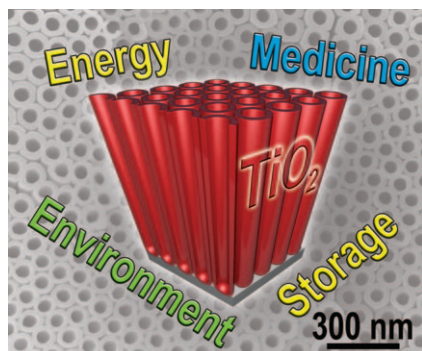


Integration of new AA members: A pyrrolysyl-tRNA synthetase:tRNA pair can be combined with an orthogonal pair from *Methanocaldococcus jannaschii* to incorporate two chemically distinct noncanonical amino acids into a single recombinant protein. This modification was enabled by the tandem read-through of a three-base termination codon and a four-base frameshift codon at natural and orthogonal ribosomes.

For the USA and Canada:
ANGEWANDTE CHEMIE International
Edition (ISSN 1433-7851) is published weekly
by Wiley-VCH, PO Box 191161, 69451 Wein-
heim, Germany. Air freight and mailing in the
USA by Publications Expediting Inc., 200
Meacham Ave., Elmont, NY 11003. Periodicals

postage paid at Jamaica, NY 11431. US POST-
MASTER: send address changes to *Angewandte
Chemie*, Journal Customer Services, John
Wiley & Sons Inc., 350 Main St., Malden,
MA 02148-5020. Annual subscription price for
institutions: US\$ 9442/8583 (valid for print and
electronic / print or electronic delivery); for

individuals who are personal members of a
national chemical society prices are available
on request. Postage and handling charges
included. All prices are subject to local VAT/
sales tax.



A new escapade for titania: Titanium dioxide is one of the most studied materials and has many applications, for example in photocatalysis, dye-sensitized solar cells, and biomedical devices. TiO_2 nanotubes, which have outstanding properties and have resulted in much research interest, play a particularly important part.

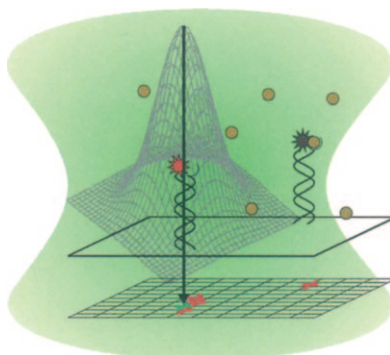
Reviews

Nanoscience

P. Roy, S. Berger,
P. Schmuki* ————— 2904 – 2939

TiO_2 Nanotubes: Synthesis and Applications

Revolution in resolution: Abbe's resolution limit has been overcome in fluorescence microscopy by using light-driven processes to switch the emission of fluorophores on and off. Alternatively, chemical reactions can be used, for example the coordination of Cu^{2+} ions to a fluorescent probe for the stochastic switching between spectroscopic states.



Communications

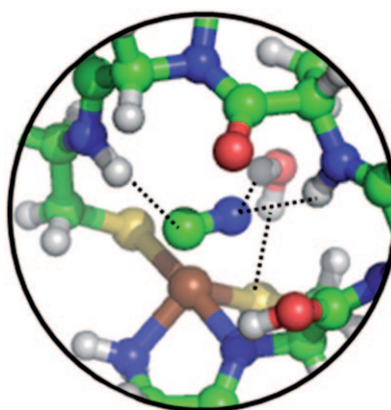
Single-Molecule Spectroscopy

M. Schwing, A. Kiel, A. Kurz,
K. Lymperopoulos, A. Sprödefeld,
R. Krämer, D.-P. Herten* — 2940 – 2945

Far-Field Nanoscopy with Reversible Chemical Reactions



Water in site: The structure of a stable adduct of a peptide-based nickel superoxide dismutase model (NiSOD) with cyanide as substrate analogue is determined by NMR spectroscopy and optimized by DFT methods. A functional water molecule is found in the active site (see picture; Ni brown, O red/pink, C green, N blue). The role of this water molecule in the catalytic degradation of $\text{O}_2^{\cdot-}$ is discussed.



Enzyme Catalysis

D. Tietze, S. Voigt, D. Mollenhauer,
M. Tischler, D. Imhof, T. Gutmann,
L. González, O. Ohlenschläger,
H. Breitzke, M. Görlach,
G. Buntkowsky* ————— 2946 – 2950

Revealing the Position of the Substrate in Nickel Superoxide Dismutase: A Model Study

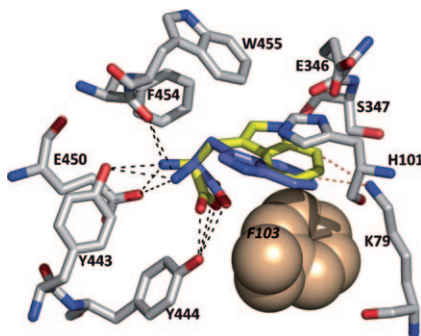


Enzymatic Halogenation

A. Lang, S. Polnick, T. Nicke, P. William, E. P. Patallo, J. H. Naismith, K.-H. van Pée* — 2951 – 2953



Changing the Regioselectivity of the Tryptophan 7-Halogenase PrnA by Site-Directed Mutagenesis



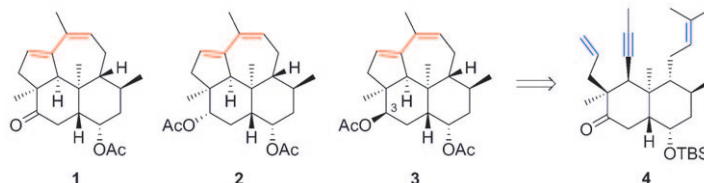
Creating more space in the active site of the tryptophan 7-halogenase PrnA by exchanging the large amino acid phenylalanine for the smaller alanine makes it possible for the substrate to bind in different orientations (see picture; yellow PrnA, blue PrnAF103A variant). This results in halogenation of the differently bound substrate in the 5-position of the indole ring.

Diterpenes

M. Schubert, P. Metz* — 2954 – 2956



Enantioselective Total Synthesis of the Diterpenes Kempene-2, Kempene-1, and 3-*epi*-Kempene-1 from the Defense Secretion of Higher Termites



Two rings in one sweep: A domino meta-thesis of the bicyclic dienyne **4** (TBS = *tert*-butyldimethylsilyl) obtained from a catalytic enantioselective Diels–Alder reaction

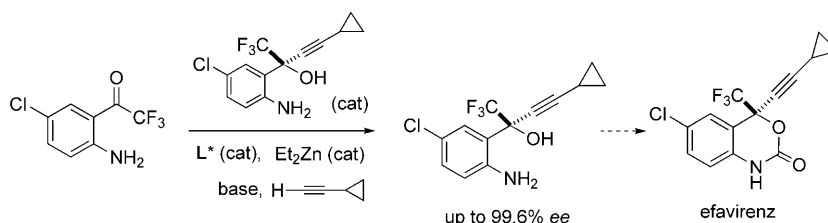
as the key process enabled the efficient preparation of the tetracyclic diterpenes kempene-2 (**1**), kempene-1 (**2**), and 3-*epi*-kempene-1 (**3**).

Alkynylzinc Addition

N. Chinkov, A. Warm, E. M. Carreira* — 2957 – 2961



Asymmetric Autocatalysis Enables an Improved Synthesis of Efavirenz



Priming the pump: An asymmetric autocatalytic zinc acetylide addition employs catalytic amounts of the enantiomerically pure product as part of a chiral cocktail.

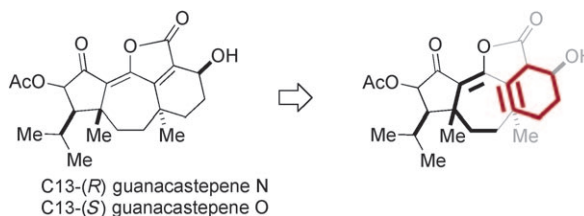
This new strategy enables an improved synthesis of a key precursor to efavirenz (see scheme).

Cyclohexyne in Total Synthesis

C. M. Gampe, E. M. Carreira* — 2962 – 2965

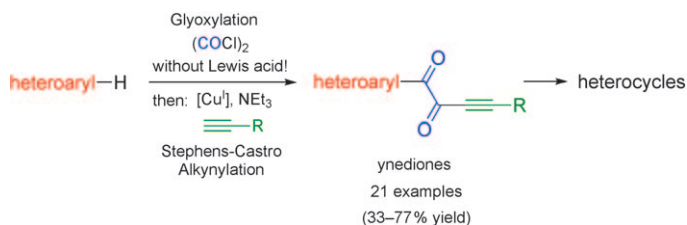


Total Syntheses of Guanacastepenes N and O



The cycloinsertion of cyclohexyne into a pentalene has provided access to the carbon scaffold of the guanacastepenes in nine steps. A late-stage diversifying ox-

idation of the core structure enabled the synthesis of guanacastepene N and the first total synthesis of guanacastepene O.



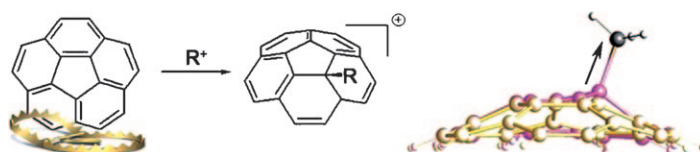
One step back, two steps forward! Starting from diverse heterocycles, the title reaction furnishes ynediones under very mild conditions in a direct and preparatively simple one-pot process. The key to avoiding decarbonylation is the Cu^I -cata-

lyzed Stephens–Castro alkynylation rather than the usually more efficient Sonogashira coupling. In addition, novel highly atom-economical four-component syntheses of various heterocycles can be achieved.

Heterocycle Synthesis

E. Merkul, J. Dohe, C. Gers, F. Rominger, T. J. J. Müller* 2966–2969

Three-Component Synthesis of Ynediones by a Glyoxylation/Stephens–Castro Coupling Sequence



Trap for electrophiles: The reaction of corannulene with halogenated hydrocarbons in the presence of AlCl_3 gave the products of an electrophilic attack on the hub carbon atom of the curved aromatic

surface (see picture). The X-ray diffraction characterization of a series of bowl-shaped cations illustrates structural deformations caused by the site-directed interior surface functionalization.

Carbocations

A. V. Zabula, S. N. Spisak, A. S. Filatov, A. Y. Rogachev, M. A. Petrukhina* 2971–2974

A Strain-Releasing Trap for Highly Reactive Electrophiles: Structural Characterization of Bowl-Shaped Arenium Carbocations



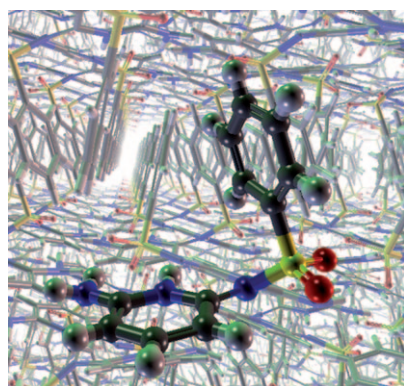
With our compliments: The 1,3-dicarbonyl unit has been shown to be a new and useful leaving group for iron-catalyzed bond cleavage (see scheme). This new

strategy can complement the traditional Friedel–Crafts reaction and was applied in the synthesis of indene derivatives.

Synthetic Methods

H. Li, W. Li, W. Liu, Z. He, Z. Li* 2975–2978

An Efficient and General Iron-Catalyzed C–C Bond Activation with 1,3-Dicarbonyl Units as a Leaving Groups



The tale of Molecule VI: Past failures to predict the polymorphs of a sulfonamide using molecular mechanics have led to speculation that crystal-structure prediction may be of limited use owing to the kinetic nature of crystallization. An approach based on quantum mechanics now successfully predicts the three known polymorphs of this compound (molecule VI, see structure). Accurate lattice energy calculations are thus sufficient to predict the polymorphs of small organic molecules.

Crystal-Structure Prediction

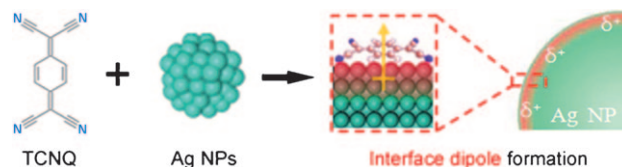
H. C. S. Chan, J. Kendrick, F. J. J. Leusen* 2979–2981

Molecule VI, a Benchmark Crystal-Structure-Prediction Sulfonamide: Are Its Polymorphs Predictable?



Olefin Separation

I. S. Chae, S. W. Kang, J. Y. Park, Y.-G. Lee,
J. H. Lee, J. Won,
Y. S. Kang* — 2982–2985



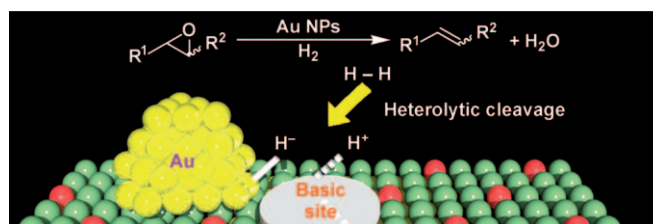
Surface Energy-Level Tuning of Silver Nanoparticles for Facilitated Olefin Transport

Calling the tune: High positive surface charges induced by tetracyanoquinodimethane (TCNQ) allow tuning of the energy levels of silver nanoparticles (AgNPs) through an interface dipole (see

picture). Facilitated transport membranes containing AgNPs with TCNQ dispersed in poly(vinylpyrrolidone) show high mixed-gas selectivity for the separation of olefin/paraffin mixtures.

Heterogeneous Catalysis

A. Noujima, T. Mitsudome, T. Mizugaki,
K. Jitsukawa, K. Kaneda* — 2986–2989



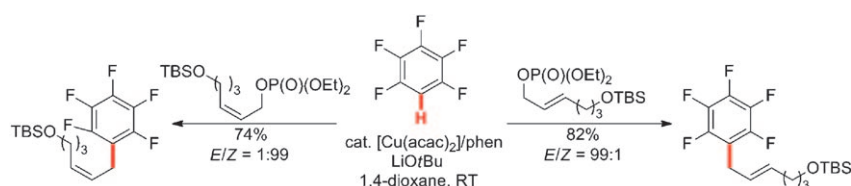
Selective Deoxygenation of Epoxides to Alkenes with Molecular Hydrogen Using a Hydrotalcite-Supported Gold Catalyst: A Concerted Effect between Gold Nanoparticles and Basic Sites on a Support

A picky catalyst: Hydrotalcite-supported gold nanoparticles (Au/HT) efficiently catalyze the deoxygenation of epoxides to alkenes using molecular hydrogen as an ideal reductant. Various epoxides have

been deoxygenated to the corresponding alkenes (see picture) with over 99% selectivity. The high selectivity is based on the concerted effect between basic sites of HT and the gold nanoparticles.

C–H Functionalization

T. Yao, K. Hirano,* T. Satoh,
M. Miura* — 2990–2994



Stereospecific Copper-Catalyzed C–H Allylation of Electron-Deficient Arenes with Allyl Phosphates

Rapid and concise: The title reaction proceeds via copper complexes in a highly stereospecific manner (see scheme; acac = acetylacetonate, phen = 1,10-phenanthroline, TBS = *t*BuMe₂Si). The catalysis

provides a rapid and concise route to allylarenes that contain fluorinated aromatic cores of an electron-deficient nature.

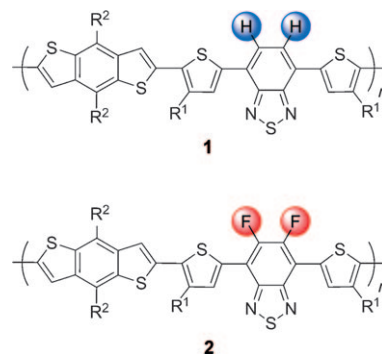
Solar Cells

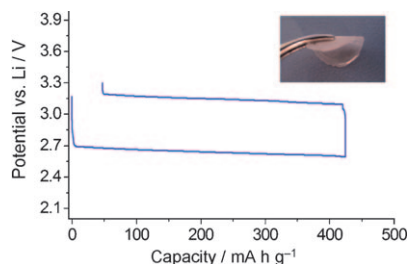
H. Zhou, L. Yang, A. C. Stuart, S. C. Price,
S. Liu, W. You* — 2995–2998



Development of Fluorinated Benzothiadiazole as a Structural Unit for a Polymer Solar Cell of 7% Efficiency

High-powered polymer: Fluorinated benzothiadiazole was incorporated into a polymer that was used in a high-performance solar cell. The model polymer **2** has decreased HOMO and LUMO energy levels and a similar band gap when compared with its nonfluorinated analogue **1**. A bulk heterojunction device derived from **1** demonstrated a high power conversion efficiency of 7.2% (5.0% for **1**).



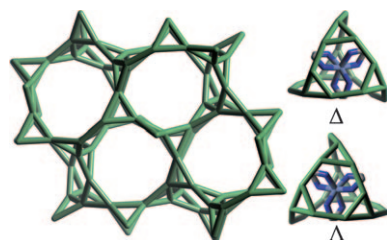


A polymer makes it possible: Use of an advanced polymer electrolyte allowed clarification of the oxygen reaction mechanism in lithium–air solid-state batteries. The related reversible processes are identified to occur at potential values that are the lowest ever reported in the absence of catalyst.

Electrochemical Cells

J. Hassoun, F. Croce, M. Armand, B. Scrosati* — 2999 – 3002

Investigation of the O₂ Electrochemistry in a Polymer Electrolyte Solid-State Cell

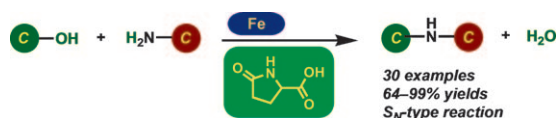


A new zeotype structure with 3D intersecting 10-ring channels is found in [Ni(en)₃][Ga₂Ge₄O₁₂] (denoted GaGeO-CJ63, en = ethylenediamine). Its framework (see picture) is constructed exclusively by 3-rings, and the framework density is the second lowest among all known zeolite structures. One of the two kinds of cages in GaGeO-CJ63 is chiral and its chirality comes from the Δ and Λ enantiomers of occluded [Ni(en)₃]²⁺.

Zeolite Analogues

Y. Han, Y. Li, J. Yu,* R. Xu — 3003 – 3005

A Gallogermanate Zeolite Constructed Exclusively by Three-Ring Building Units



Ironing it out: The straightforward N-alkylation using alcohols and iron/amino acid catalysis is described (see scheme). The reaction does not proceed by the conventional “borrowing hydrogen” mechanism, but appears to involve a

substitution pathway (S_N) at the sp³ carbon atom bearing the hydroxy group of the alcohol. Developing a catalyst that is effective at a near neutral pH was key to the successful N-alkylation.

N-alkylation

Y. Zhao, S. W. Foo, S. Saito* — 3006 – 3009

Iron/Amino Acid Catalyzed Direct N-Alkylation of Amines with Alcohols



A Fischer carbene complex within the N-heterocyclic carbene skeleton is present in Mn^I/Au^I heterometallic compounds that were synthesized from an acyclic diamine-carbene complex, through a transloca-

tion process of metallic ions under basic conditions and subsequent alkylation with methyl triflate (see scheme; bipy = bipyridyl, [Mn] = [Mn(CO)₂(bipy)]).

Carbene Ligands

J. Ruiz,* L. García, B. F. Perandones, M. Vivanco — 3010 – 3012

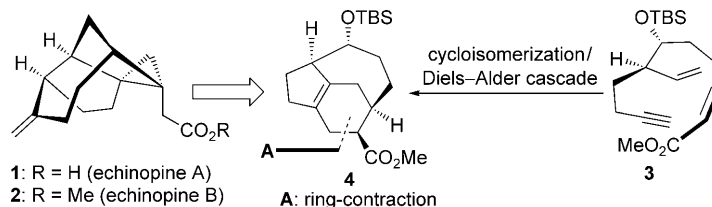
A Fischer Carbene within an Arduengo Carbene

Natural Products

P. A. Peixoto, R. Severin, C.-C. Tseng,
D. Y.-K. Chen* 3013–3016



Formal Asymmetric Synthesis of
Echinopine A and B



Enticing structures: The formal syntheses of **1** and **2** were accomplished by using a cascade strategy involving an enyne cycloisomerization reaction and an intramolecular Diels–Alder reaction starting from **3**. The resulting **4** underwent a late-

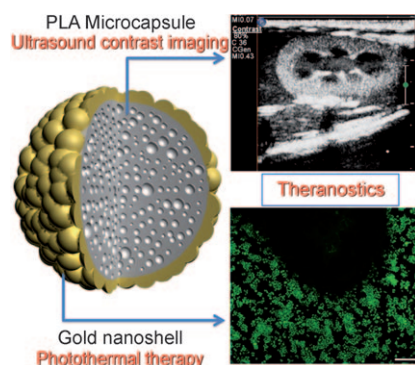
stage ring contraction to enable the preparation of a reported advanced intermediate, thereby constituting a formal synthesis of the structurally intriguing title compounds.

Theranostic Agents

H. T. Ke, J. R. Wang, Z. F. Dai,* Y. S. Jin,
E. Z. Qu, Z. W. Xing, C. X. Guo, X. L. Yue,
J. B. Liu 3017–3021



Gold-Nanoshelled Microcapsules:
A Theranostic Agent for Ultrasound
Contrast Imaging and Photothermal
Therapy



A valuable shell: The combination of electrostatic deposition of gold nanoparticles onto microcapsules and a surface seeding method results in the formation of gold nanoshells (see picture). This nano/microcomposite is able to operate as a theranostic agent for both contrast-enhanced ultrasonic imaging (diagnostic) and photothermal therapy (therapeutic), and thus holds a great potential for photothermal therapy in cancer treatment.

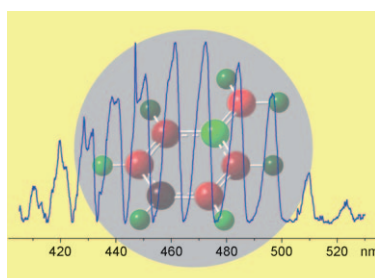


Aromatic Cations

A. Nagy, J. Fulara, I. Garkusha,
J. P. Maier* 3022–3025



On the Benzylium/Tropylium Ion
Dichotomy: Electronic Absorption
Spectra in Neon Matrices



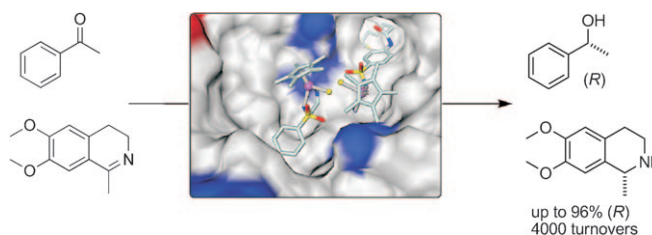
Benzyl and tropyli in charge: Electronic spectra of mass-selected benzylium (Bz^+) and tropylium (Tr^+) cations embedded in solid neon are reported for the first time. They reveal a weak $(1)^1B_1 \leftarrow X^1A_1$ visible (see picture) and a much stronger $(1)^1A_1 \leftarrow X^1A_1$ ultraviolet transition for Bz^+ (C_{2v} symmetry). The lowest dipole-allowed $^1A''_2 \leftarrow X^1A_1$ absorption in the ultraviolet region for Tr^+ (D_{7h}) is also observed.

Artificial Metalloenzyme

M. Dürrenberger, T. Heinisch,
Y. M. Wilson, T. Rossel, E. Nogueira,
L. Knörr, A. Mutschler, K. Kersten,
M. J. Zimbron, J. Pierron, T. Schirmer,
T. R. Ward* 3026–3029



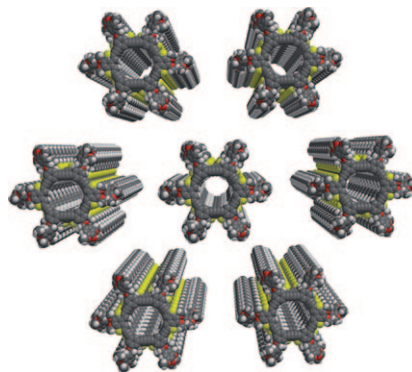
Artificial Transfer Hydrogenases for the
Enantioselective Reduction of Cyclic
Imines



Man-made activity: Introduction of a biotinylated iridium piano stool complex within streptavidin affords an artificial imine reductase (see scheme). Saturation mutagenesis allowed optimization of the

activity and the enantioselectivity of this metalloenzyme, and its X-ray structure suggests that a nearby lysine residue acts as a proton source during the transfer hydrogenation.

Take the tube: Self-organization of shape-persistent macrocycles in the liquid-crystalline phase by π - π stacking leads to empty nanochannels that have an inner diameter above one nanometer and either tight or more permeable walls (see picture). Solid-state NMR spectroscopy was used to confirm that the channels do not contain solvent molecules or alkyl chains.



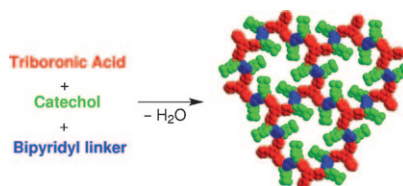
Macrocycles

M. Fritzsche, A. Bohle, D. Dudenko,
U. Baumeister, D. Sebastiani, G. Richardt,
H. W. Spiess, M. R. Hansen,*
S. Höger* _____ 3030–3033

Empty Helical Nanochannels with
Adjustable Order from Low-Symmetry
Macrocycles



The BN connection: Crystalline and soft molecular networks can be constructed using dative B–N bonds (see picture). The networks are obtained in a one-step, three-component reaction involving a triboronic acid, a catechol, and a bipyridyl linker.



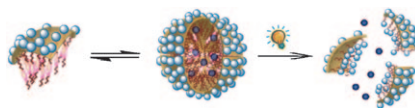
Supramolecular Chemistry

E. Sheepwash, V. Krampl, R. Scopelliti,
O. Sereda, A. Neels,
K. Severin* _____ 3034–3037

Molecular Networks Based on Dative
Boron–Nitrogen Bonds



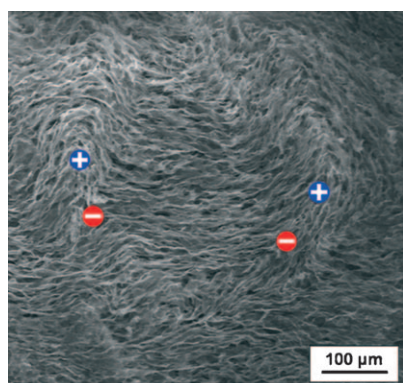
Supramolecular disassembly: Phototriggered release of noncovalently sequestered lipophilic guest molecules from dendritic supramolecular assemblies has been demonstrated. Facially amphiphilic dendrimers have been shown to provide a unique opportunity to fine-tune the release kinetics of the guest molecules in response to light (see picture).



Dendritic Micelles

V. Yesilyurt, R. Ramireddy,
S. Thayumanavan* _____ 3038–3042

Photoregulated Release of Noncovalent
Guests from Dendritic Amphiphilic
Nanocontainers



Crystal clear: The liquid crystallinity of graphene oxide platelets in aqueous dispersion is demonstrated. Graphene oxide sheets are arranged around liquid-crystal disclinations (see picture). The orientation of the liquid crystals can be manipulated by a magnetic field or mechanical deformation.

Liquid Crystals

J. E. Kim, T. H. Han, S. H. Lee, J. Y. Kim,
C. W. Ahn, J. M. Yun,
S. O. Kim* _____ 3043–3047

Graphene Oxide Liquid Crystals

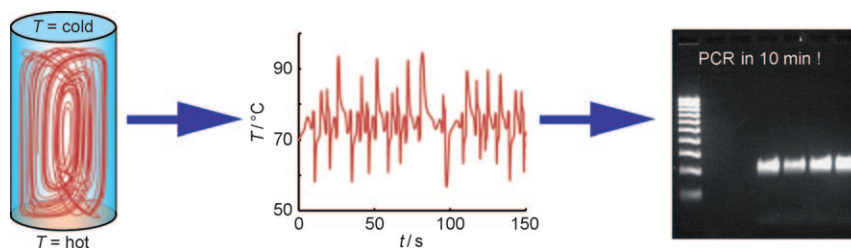


Microreactors

R. Muddu, Y. A. Hassan,
V. M. Ugaz* ————— 3048 – 3052



Chaotically Accelerated Polymerase Chain Reaction by Microscale Rayleigh–Bénard Convection



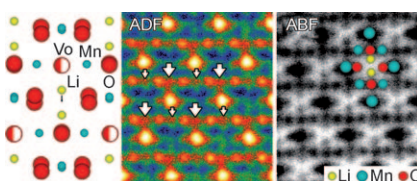
Going with the flow: DNA replication by the polymerase chain reaction (PCR) can proceed at a greatly accelerated rate when performed in the presence of a chaotic flow induced by microscale thermal con-

vection (see picture). The consequences of these effects sharply contradict established design rules for chemistry involving coupled flow and reaction.

Electron Microscopy

R. Huang, Y. H. Ikuhara, T. Mizoguchi,
S. D. Findlay, A. Kuwabara, C. A. J. Fisher,
H. Moriwake, H. Oki, T. Hirayama,
Y. Ikuhara* ————— 3053 – 3057

Oxygen-Vacancy Ordering at Surfaces of Lithium Manganese(III,IV) Oxide Spinel Nanoparticles



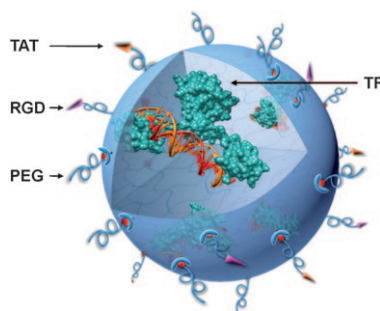
Direct observation of light elements (Li and O) in oxygen-deficient lithium manganese spinel by spherical aberration-corrected scanning transmission electron microscopy is reported. A previously unknown ordered structure was revealed by annular dark-field (ADF) imaging of oxygen columns, while Li ions are visualized successfully by annular bright-field (ABF) imaging (see picture).



Protein Delivery

Y. Liu, H. Wang,* K. Kamei, M. Yan,
K.-J. Chen, Q. Yuan, L. Shi,* Y. Lu,*
H.-R. Tseng* ————— 3058 – 3062

Delivery of Intact Transcription Factor by Using Self-Assembled Supramolecular Nanoparticles



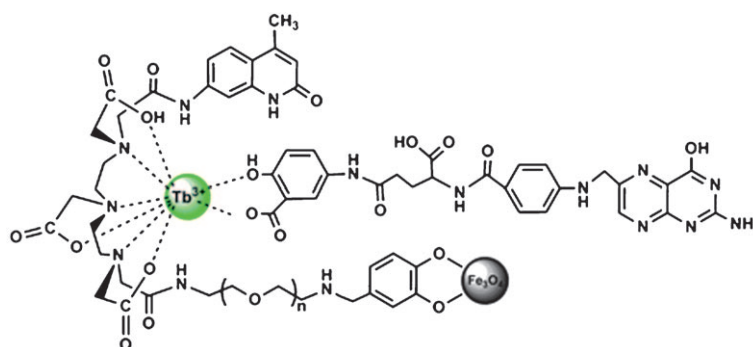
Special delivery: A supramolecular nanoparticle provides a facile and modular protein delivery system (see picture, TAT enables cell membrane penetration, RGD targeting, and PEG passivation) for highly efficient transduction of intact (unmodified) transcription factors (TF). Such a TF delivery approach provides a powerful method for manipulating cellular behavior.

Imaging Agents

B. Wang, J. Hai, Q. Wang, T. Li,
Z. Yang* ————— 3063 – 3066



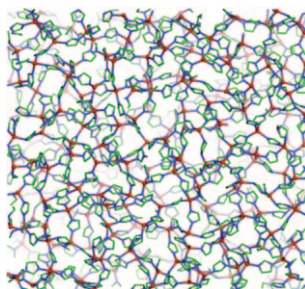
Coupling of Luminescent Terbium Complexes to Fe₃O₄ Nanoparticles for Imaging Applications



Dual imaging agent: A fluorescent Tb^{III} complex coupled to Fe₃O₄ nanoparticles and bearing a folic acid residue (see picture) shows superparamagnetism, low cytotoxicity, and high cell uptake, and thus

can be used for in vitro fluorescence and magnetic resonance imaging of cells that overexpress the folate receptor, such as HeLa cells.

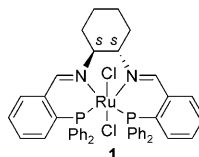
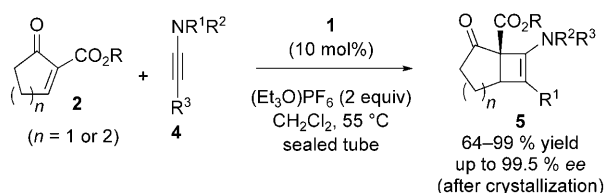
Each the same: A stable, recoverable, amorphous phase (see topology model) was produced by heating each of four different zeolitic imidazolate frameworks ZIF-1, -3, -4, and Co-ZIF-4. By comparing nanoindentation results, density measurements, and X-ray total scattering results, it is concluded that the structure of the amorphous phase is equivalent in each case. Amorphization was only observed in ZIFs encompassing unsubstituted imidazolate ligands.



Metal–Organic Frameworks

T. D. Bennett, D. A. Keen, J. C. Tan, E. R. Barney, A. L. Goodwin, A. K. Cheetham* — 3067–3071

Thermal Amorphization of Zeolitic Imidazolate Frameworks



Asymmetric Catalysis

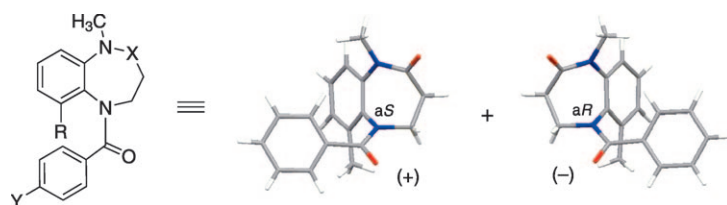
C. Schötes, A. Mezzetti* — 3072–3074

Enantioselective Ficini Reaction: Ruthenium/PNNP-Catalyzed [2+2] Cycloaddition of Ynamides with Cyclic Enones



Chiral cyclobuteneamides made easy: Double chloride abstraction from the ruthenium/PNNP complex **1** in the presence of unsaturated β -keto esters **2** gives the dicationic adducts $[\text{Ru}(\text{2})(\text{PNNP})]^{2+}$

(**3**) that catalyze the [2+2] cycloaddition of a variety of ynamides **4** to produce cyclobuteneamides **5** with high yield and enantioselectivity (see scheme).



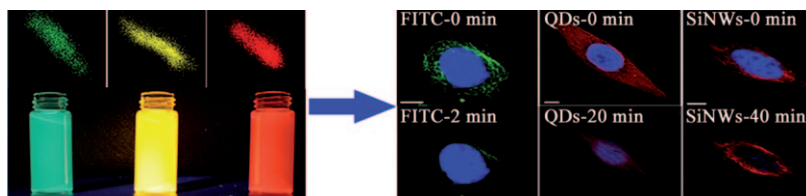
Latent chirality: Atropisomerism in the vaptan class of vasopressin receptor ligands with *N*-benzoyl benzo-fused seven-membered-ring nitrogen heterocycles was investigated by freezing the axis by *ortho* substitution. The aS/aR atropisomers

caused by the $\text{Ar}-\text{N}(\text{=CO})$ axis were separated to reveal that the vasopressin receptor recognizes the *cis,aS* conformation (see picture; $\text{R} = \text{CH}_3$, $\text{X} = -\text{CO}-$, $\text{Y} = \text{H}$) when it binds to the ligand.

Atropisomerism

H. Tabata, J. Nakagomi, D. Morizono, T. Oshitari, H. Takahashi, H. Natsugari* — 3075–3079

Atropisomerism in the Vaptan Class of Vasopressin Receptor Ligands: The Active Conformation Recognized by the Receptor



All aglow: Multicolored fluorescent quantum-dot (QD)-decorated silicon nanowires (SiNWs) are easily prepared by a one-pot microwave-assisted synthesis. The as-prepared SiNWs are highly lumi-

nescent (see picture, left) and are well-suited to long-term immunofluorescent cellular imaging (see stability comparison, right).

Fluorescent Probes

Y. He,* Y. L. Zhong, F. Peng, X. P. Wei, Y. Y. Su, S. Su, W. Gu, L. S. Liao, S. T. Lee* — 3080–3083

Highly Luminescent Water-Dispersible Silicon Nanowires for Long-Term Immunofluorescent Cellular Imaging



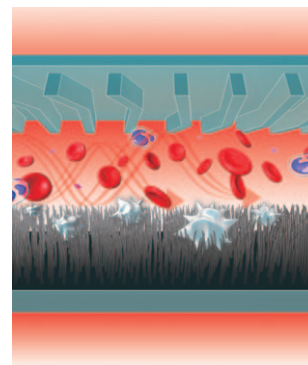
Cell Capture

S. T. Wang, K. Liu, J. Liu, Z. T.-F. Yu, X. Xu, L. Zhao, T. Lee, E. K. Lee, J. Reiss, Y.-K. Lee, L. W. K. Chung, J. Huang, M. Rettig, D. Seligson, K. N. Duraiswamy,* C. K.-F. Shen,* H.-R. Tseng* **3084–3088**



Highly Efficient Capture of Circulating Tumor Cells by Using Nanostructured Silicon Substrates with Integrated Chaotic Micromixers

Finding a needle in a haystack: A new technology is demonstrated to enrich circulating tumor cells (CTCs) with high efficiency by integrating an antibody-coated silicon nanopillar (SiNP, see picture; gray) substrate with an overlaid polydimethylsiloxane (PDMS) microfluidic chaotic mixer (turquoise). It shows significantly improved sensitivity in detecting rare CTCs from whole blood, thus providing an alternative for monitoring cancer progression.



Supporting information is available on www.angewandte.org (see article for access details).



A video clip is available as Supporting Information on www.angewandte.org (see article for access details).



This article is available online free of charge (Open Access)

Angewandte InterScience®
DISCOVER SOMETHING GREAT

“Hot Papers” are chosen by the Editors for their importance in a rapidly evolving field of high current interest. A preview with the graphical abstracts of these articles can be found on the *Angewandte Chemie* homepage in Wiley InterScience at www.angewandte.org.

All articles in *Angewandte Chemie* are published online several weeks ahead of print. They are found under the “EarlyView” link on the journal’s homepage in Wiley InterScience.

Service

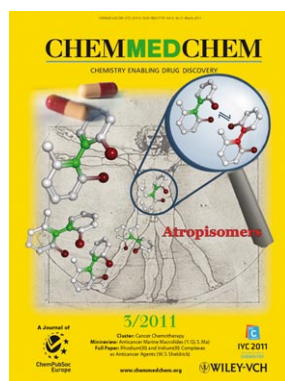
Spotlight on Angewandte's Sister Journals _____ **2876–2878**

Preview _____ **3089**

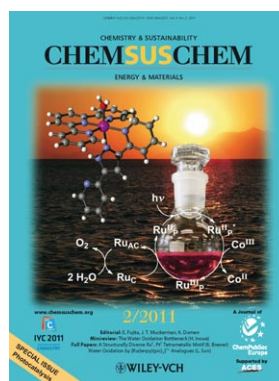
Check out these journals:



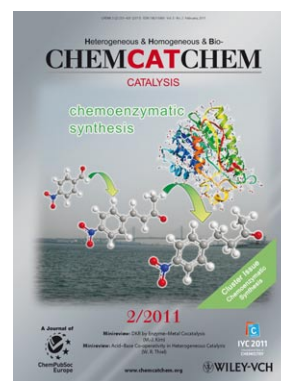
www.chemasianj.org



www.chemmedchem.org



www.chemsuschem.org



www.chemcatchem.org